EBioMedicine 16 (2017) 238–250

Contents lists available at ScienceDirect

EBioMedicine

journal homepage: www.ebiomedicine.com

Research Paper

Angiotensin-II-induced Muscle Wasting is Mediated by 25-Hydroxycholesterol via GSK3β Signaling Pathway

Congcong Shen [a,1], Jin Zhou [b,**,1], Xiaoxiao Wang [a,1], Xi-Yong Yu [c,1], Chun Liang [d,1], Bin Liu [e,1], Xiangbin Pan [f,1], Qiong Zhao [a], Jenny Lee Song [a], Jiajun Wang [g], Meiyu Bao [a], Chaofan Wu [a], Yangxin Li [h,**], Yao-Hua Song [a,*]

[a] Cyrus Tang Hematology Center, Collaborative Innovation Center of Hematology, Soochow University, Suzhou, PR China
[b] Department of General Surgery, The First Affiliated Hospital of Soochow University, Suzhou, PR China
[c] Guangdong Cardiovascular Institute, Guangzhou Medical University, Guangzhou, Guangdong, PR China
[d] Department of Cardiology, Shanghai Changzheng Hospital, Second Military Medical University, No. 415, Fengyang Road, Shanghai, PR China
[e] Cardiovascular Disease Center, The First Hospital of Ji Lin University, Changchun, Jilin 130021, PR China
[f] Department of Cardiac Surgery, Fuwai Hospital, PR China
[g] Department of Gynecology, The Affiliated Maternity and Child Health Hospital of Nanjing Medical University, Wuxi, PR China
[h] The Department of Cardiovascular Surgery of the First Affiliated Hospital and the Institute for Cardiovascular Science, Soochow University, Suzhou, Jiangsu 215123, PR China

ARTICLE INFO

Article history:
Received 28 July 2016
Received in revised form 20 January 2017
Accepted 27 January 2017
Available online 30 January 2017

Keywords:
Cardiac cachexia
Heart failure
TNF-α
Angiotensin II
Ch25h

ABSTRACT

While angiotensin II (ang II) has been implicated in the pathogenesis of cardiac cachexia (CC), the molecules that mediate ang II's wasting effect have not been identified. It is known TNF-α level is increased in patients with CC, and TNF-α release is triggered by ang II. We therefore hypothesized that ang II induced muscle wasting is mediated by TNF-α. Ang II infusion led to skeletal muscle wasting in wild type (WT) but not in TNF alpha type 1 receptor knockout (TNFR1KO) mice, suggesting that ang II induced muscle loss is mediated by TNF-α through its type 1 receptor. Microarray analysis identified cholesterol 25-hydroxylase (Ch25h) as the down stream target of TNF-α. Intraperitoneal injection of 25-hydroxycholesterol (25-OHC), the product of Ch25h, resulted in muscle loss in C57BL/6 mice, accompanied by increased expression of atrogin-1, MuRF1 and suppression of IGF-1/Akt signaling pathway. The identification of 25-OHC as an inducer of muscle wasting has implications for the development of specific treatment strategies in preventing muscle loss.

1. Introduction

About 1/3 of patients with congestive heart failure suffer from cardiac cachexia (CC), which is characterized by muscle weakness and atrophy (Khawaja et al., 2014; Mancini et al., 1992; von Haehling et al., 2007). Patients with CC have a poor prognosis and there is no effective treatment for this condition, mainly due to the fact that mechanisms involved in CC remain largely unknown.

Clinical studies show that ang II is increased in patients with CC. We and others have shown that ang II infusion induces muscle wasting in rodents. However, ang II receptors are expressed at very low levels in adult skeletal muscle. Therefore, ang II induced muscle wasting may be mediated by other intermediate factors. It is well documented that TNF-α levels are increased in patients with CC (Cicoira et al., 2001; Doehner et al., 2007; Toth et al., 2006; Yende et al., 2006). In monocrotaline induced rat heart failure model, myocyte apoptosis and muscle atrophy are associated with increased levels of ang II and TNF-α (Dalla Libera et al., 2001). Blockade of ang II type 1 receptor with irbesartan prevented the increase of plasma TNF-α levels and inhibited muscle atrophy (Dalla Libera et al., 2001). Despite the correlation between ang II and TNF-α, no studies to date have examined this relationship directly to determine whether ang II induced muscle wasting is mediated by TNF-α.

TNF-α has two receptors, TNFR1 and TNFR2. Previous studies suggest that TNF-α induced muscle wasting is mediated by TNFR1 (Hardin et al., 2008; Llovera et al., 1998). We therefore took advantage of the TNFR1 knockout mouse model (TNFR1KO) to directly test the hypothesis that loss of TNFR1 would prevent ang II induced muscle wasting. We demonstrated that ang II induced muscle wasting is mediated by TNF-α through TNFR1. Furthermore, we identified Ch25h as the downstream target of TNF-α that mediate ang II's wasting effect. Ch25h

Abbreviations: ang II, angiotensin II; CC, cardiac cachexia; Ch25h, 25-hydroxylase; WT, wild type; TNFR1KO, TNF alpha type 1 receptor knockout; 25-OHC, 25-hydroxycholesterol; 20-OHC, 20α-hydroxycholesterol; 22-OHC, 22(R)-hydroxycholesterol; IR, ischemia reperfusion injury; CSA, cross sectional area.

* Correspondence to: Yao-Hua Song, Cyrus Tang Hematology Center, Collaborative Innovation Center of Hematology, Soochow University, 199 Ren Ai Road, Suzhou 215123, PR China.
** Corresponding authors.
E-mail addresses: 13913506369@163.com (J. Zhou), yangxin_li@yahoo.com (Y. Li), yaohua_song1@yahoo.com (Y.-H. Song).
[1] These authors contributed equally to this work.

http://dx.doi.org/10.1016/j.ebiom.2017.01.040

is an enzyme that convert cholesterol into 25-hydroxycholesterol (25-OHC), which has been shown to inhibit myogenesis via down regulation of IGF-1 signaling (Romanelli et al., 2009). We showed that intraperitoneal injection of 25-OHC resulted in muscle loss in C57BL/6 mice, accompanied by increased expression of atrogin-1, MuRF1 and suppression of IGF-1/Akt signaling and reduced phosphorylation of GSK3-beta. Our data suggest that ang II infusion activates TNF/25-OHC pathway, leading to increased expression of markers of proteolysis, apoptosis and impaired myogenesis through GSK3-beta activation.

2. Materials and Methods

2.1. Mice

Male C57BL/6 mice from Model Animal Research Center of Nanjing, and TNFR1 knockout (TNFR1KO) mice from Jackson Lab were maintained in a Special Pathogen Free animal facility at Soochow University. All animal experiments comply with the ARRIVE guidelines and are carried out in accordance with the National Institutes of Health guide for the care and use of Laboratory animals (NIH Publications No. 8023, revised 1978) and the manuscript has followed such guidelines. All animal protocols were approved by the Institutional Laboratory Animal Care and Use Committee of Soochow University.

2.2. Angiotensin II Infusion Model

Osmotic minipumps (ALZET model 1007D, ALZA Corp) were implanted to infuse angiotensin II at a rate of 500 ng/kg/min or diluent as described previously (Song et al., 2005). Seven days after implantation of the osmotic pumps, mice were anesthetized and muscles were removed, weighed, and snap-frozen and stored at −80 °C until processed.

2.3. Muscle Force Measurement

Mouse grip strength was measured daily for 3 consecutive days using a Grip Strength Meter (Ji-Nan Biotechnology, ShanDong, China). Each day, 5 grip strengths were assessed at 1 min intervals, and the average grip strength over 3 days was calculated.

2.4. In Vivo Delivery of Hydroxycholesterols

25-Hydroxycholesterol (25-OHC, Sigma, Cat# H1015), 20α-hydroxycholesterol (20-OHC, Sigma, Cat# H6378) and 22(R)-hydroxycholesterol (22-OHC, Sigma, Cat# H9384), dissolved in 0.3% ethanol, were injected to C57BL/6 mice daily for 7 days (40 μg/mouse, i.p.). Control mice were injected with 0.3% ethanol.

2.4.1. Tibialis Anterior (TA) Muscle Injection of Lentivirus Overexpressing Ch25h

The mice were anesthetized. Each TA muscle was injected with 50 μl of concentrated viral preparations (7.0×10^7 transducing units/ml). The contralaterol TA muscles were injected with lentivirus carrying empty vector.

2.4.2. GSK3β Inhibitor TDZD-8 Treatment

Two hours before ang II infusion, the mice were injected with either TDZD-8 (Sigma, Cat# T8325, 5 mg/kg, 10% DMSO in PBS) or PBS containing 10% DMSO.

2.4.3. C2C12 Cell Culture

The mouse myoblast cell line C2C12 (ATCC Cat# CRL-1772, RRID:CVCL_0188) from American Type Culture Collection (Manassas, VA) was cultured in DMEM (ThermoFisher Scientific) containing 10% fetal bovine serum (FBS), 100 U/ml penicillin and 100 μg/ml streptomycin in 5% CO_2 at 37 °C. To induce differentiation, DMEM containing 2% horse serum (Gibco, Cat# 16050122) was added to C2C12 cells when the density of cells reached 70–80%.

2.4.4. Satellite Cell Isolation

TA muscles were dissected, minced and digested with Collagenase D and Dispase type II (Roche) (Liu et al., 2016). After digestion, the cells were resuspended in DMEM containing 1% glutamine and 10% FBS and plated on collagen coated dishes. Differentiation was induced by culturing the cells in DMEM containing 1% glutamine and 2% horse serum.

2.4.5. Myotube Calculation

Microscopic images of myotubes were captured using a digital camera mounted on a Leica microscope (DFC310 FX). Myotube diameter and length measurements were obtained using ImageJ software. Three short-axis measurements were taken along the length of a given myotube and averaged. The results were averaged from three independent experiments.

2.4.6. Construction of Lentivirus Overexpressing TNF-α and Ch25h

The LV5 plasmid (GenePharma, Shanghai, China) containing mouse TNF-α or Ch25h cDNA and packaging plasmids ΔR8.74, VSV-G and Rev were co-transfected into 293T cells as described previously (Zhou et al., 2014). The packaging plasmids were provided by Dr. Yun Zhao, Soochow University.

2.4.7. Microarray Analysis

C2C12 myoblasts were cultured in DMEM containing 10% FBS and then treated with TNF-α (50 ng/ml) for 24 h. In separate experiments, C2C12 cells were cultured in DMEM containing 2% horse serum for 4 days and then treated with TNF-α (50 ng/ml) for 24 h. Total RNA was extracted from C2C12 cells using Trizol reagent. RNA samples were labeled and hybridized to Affymetrix Mouse Gene 2.0 ST Array, and analyzed by Shanghai Biotechnology Corporation. The microarray data have been submitted to the NCBI Archive, under accession number GSE92671.

2.4.8. Western Blot

Proteins extracted from gastrocnemius muscles were separated by SDS-PAGE and blotted to PVDF membranes (Millipore, ISEQ00010). The following antibodies were from Cell Signaling Technology: cleaved caspase-3 (Cat# 9664 RRID:AB_2070042), GAPDH (Cat# 2118S RRID:AB_10698756), Akt (Cat# 4691S RRID:AB_915783), p-Akt (Cat#

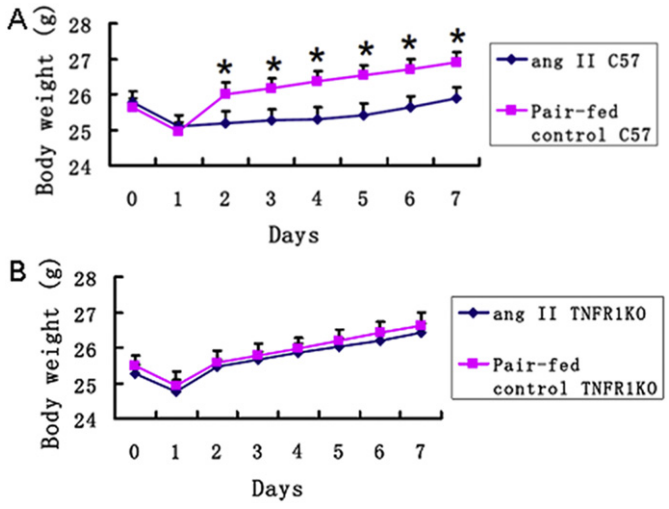

Fig. 1. TNFR1 knockout prevents ang II induced muscle wasting in mice. Changes in body weight of wild type C57BL/6 (A) and TNFR1KO mice (B) after ang II infusion for 7 days. n = 7 mice/group. P: pair-fed, sham infused mice, A: ang II infused mice. *$P < 0.01$.

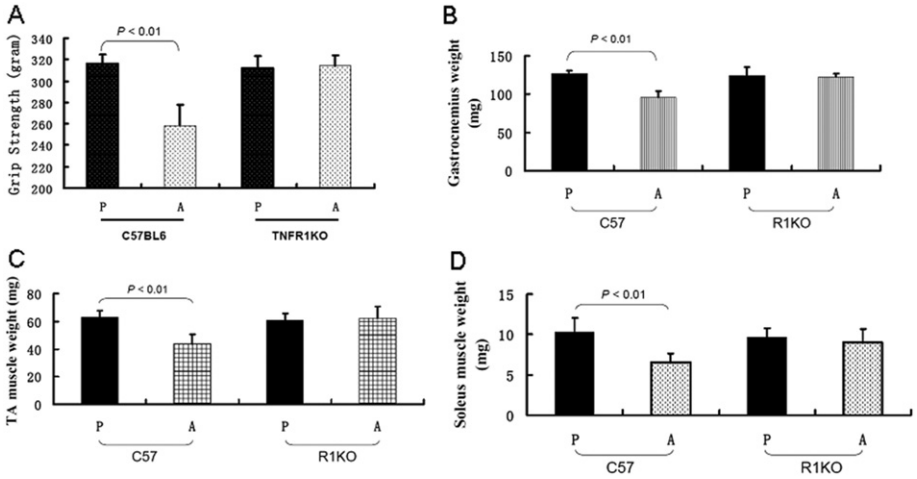

Fig. 2. Grip strength and muscle weight are maintained in ang II infused TNFR1KO mice. (A) Muscle force of each mouse was measured on three consecutive days using a Grip Strength Meter. The average muscle force (in grams) is shown (n = 7 mice/group). (B–D) Average weights of gastrocnemius, tibialis anterior (TA) and soleus muscle from both legs. C57: C57BL/6, R1KO: TNFR1 knockout. n = 7 mice/group.

4060S RRID:AB_916024), GSK3β (Cat# 9315S RRID:AB_490890), p-GSK3β (Cat# 5558S RRID:AB_10695601), Bad (Cat# 9268S RRID:AB_10695002), p-Bad (Cat# 5286S RRID:AB_2062129). The secondary antibody HRP-linked anti-rabbit IgG (Cat# A6154 RRID:AB_258284) was from Sigma. Rabbit anti-atrogin-1 (Cat# ab168372) and MuRF1 (Cat# 172479) antibodies were from Abcam.

2.4.9. Real-Time PCR

RNA was extracted using the Trizol reagent (Ambion), and cDNA was synthesized using the RevertAid First Strand cDNA Synthesis Kit (ThermoFisher Scientific). Real-time PCR was performed using the ABI 7500 Real Time PCR System with the following primers: Atrogin-1: 5′-GCAGAGAGTCGGCAAGTC3′, 5′-CAGGTCGGTGATCGTGAG3′; MuRF1: 5′-CAACCTGTGCCGCAAGTG3′, 5′-CAACCTCGTGCCTACAAGATG3′; TNF-α: 5′-CTTCTGTCTACTGAACTTCGGG3′, 5′-CAGGCTTGTCACTCGAATTTTG3′

Ch25h: 5′-CTGGGACACCATAAGGACAAG3′, 5′-AAGCCCACGTAAGTGATGATAG3′; MyoD: 5′-TGCTCCTTTGAGACAGCAGA3′, 5′-AGTAGGGAAGTGTGCGTGCT3′

18S: 5′-CTCTGTTCCGCCTAGTCCTG3′, 5′-AATGAGCCATTCGCAGTTTC3′

Relative expression was calculated from cycle threshold (Ct; relative expression = $2^{-(S\Delta Ct\ -\ C\Delta Ct)}$) values using 18S as internal control for each samples.

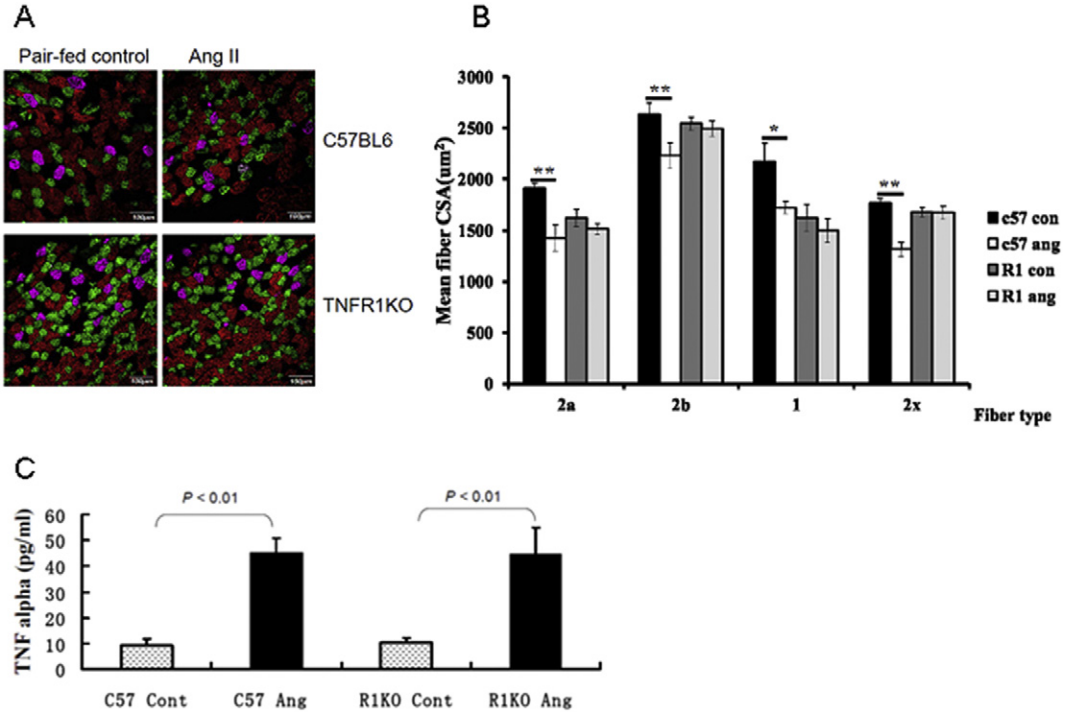

Fig. 3. Representative images of gastrocnemius muscle fiber subtype staining and mean fiber CSA. (A) Frozen sections of gastrocnemius muscles were stained with fiber type specific antibodies. Myosin heavy chain type 1 (purple), 2a (green), 2b (red) and 2× (unstained). (B) Mean myofiber cross sectional area (CSA) by fiber type. CSA was quantified using ImageJ software by an observer blinded to treatment. n = 7 mice/group. (C) Serum levels of TNF-α from mice were measured by ELISA. n = 7 mice/group. *$P < 0.05$, **$P < 0.01$.

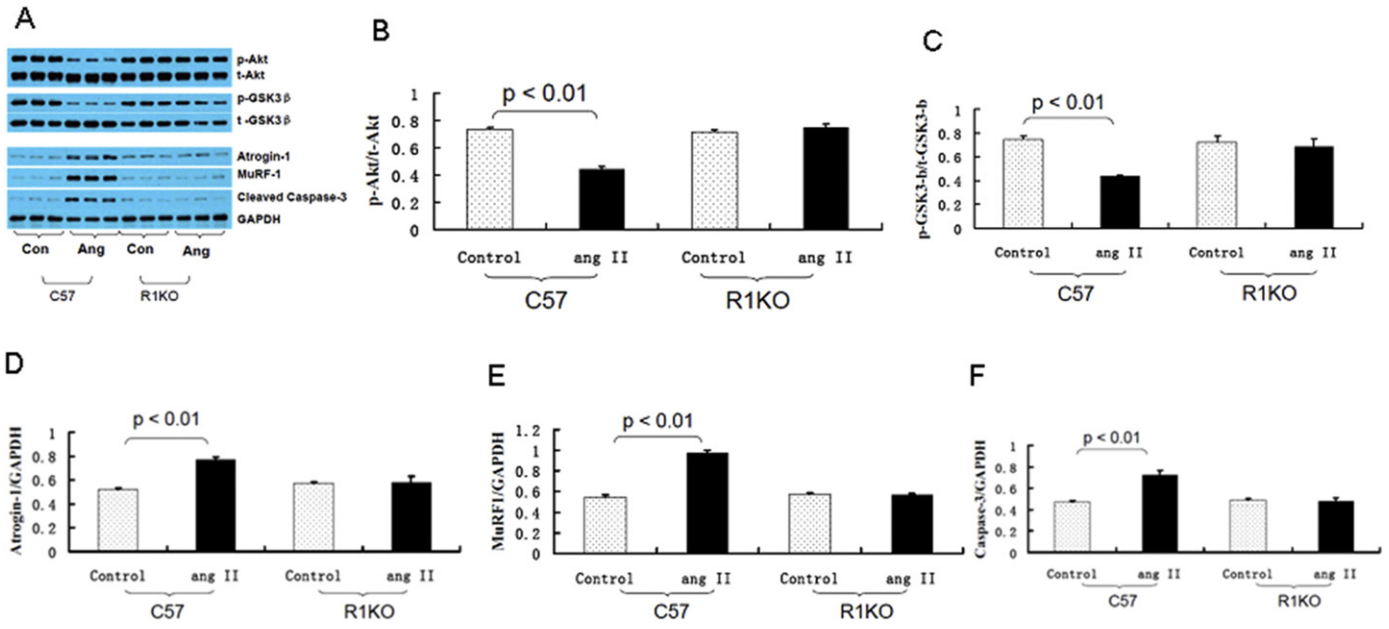

Fig. 4. Westernblot analysis of Akt, GSK3β, atrogin-1, MuRF1 and cleaved caspase-3. (A) Representative Westernblots of p-Akt, t-Akt, p-GSK3β, t-GSK3β, atrogin-1, MuRF1, cleaved caspase-3 and GAPDH expression in lysates of gastrocnemius muscles of ang II infused or pair-fed sham infused C57BL/6 (C57) or TNFR1KO mice (R1KO). (B–C) Density of p-Akt and p-GSK3β corrected for total Akt or total GSK3β, respectively, in lysates of gastrocnemius muscles (n = 3 mice/group). (D–F) Density of atrogin-1, MuRF1 and cleaved caspase-3 corrected for GAPDH in lysates of gastrocnemius muscles (n = 3 mice/group).

2.4.10. Immunostaining for MyoD, Myogenin and Pax7

Frozen sections (10 μm) were incubated with mouse anti-MyoD antibody (Thermo Fisher Scientific Cat# MA1-41017 RRID:AB_2282434) or mouse anti-myogenin (DSHB Cat# F5D RRID:AB_2146602), mouse anti-Pax7 antibody (DSHB Cat# pax7 RRID:AB_528428), and rabbit anti-laminin antibody (Sigma-Aldrich Cat# L9393 RRID:AB_477163). After washing, the sections were incubated with goat anti-mouse IgG-Alexa Fluor® 488 conjugate (Thermo Fisher Scientific Cat# A-11001 RRID:AB_2534069) or goat anti-rabbit IgG-Alexa Fluor® 568 conjugate (Thermo Fisher Scientific Cat# A11011 RRID:AB_10584650). The sections were finally incubated with DAPI to stain nuclei.

2.4.11. ELISA

Serum TNF-α and 25-OHC levels were analyzed by ELISA per manufacturer's instruction (TNF-α ELISA kit: eBioscience Cat# BMS607/3 RRID:AB_2575663, San Diego, CA; 25-OHC ELISA kit: MyBioSource Cat# MBS9310855, Inc. San Diego, CA).

2.4.12. Cross Sectional Area (CSA) of Myofibers

Gastrocnemius muscles were removed, frozen in isopentane cooled in liquid nitrogen and sectioned in a microtome cryostat.

For fiber typing, unfixed sections were incubated in antibodies against myosin heavy chain (MyHC) types 1, 2a and 2b (1:100) from Developmental Studies Hybridoma Bank (Cat# BA-D5 RRID:AB_2235587, Cat# SC-71 RRID:AB_2147165 and Cat# BF-F3 RRID:AB_2266724). MyHC type 2× expression was inferred from unstained fibers. Fluorescence-conjugated secondary antibodies to various mouse immunoglobulin subtypes from Thermo Fisher Scientific (Goat anti-Mouse IgG2b AF647, Cat# A-21242 RRID:AB_2535811, 1:250, Goat anti-Mouse IgG1 AF488, Cat# A-21121 RRID:AB_2535764, 1:500, Goat anti-Mouse IgM AF546, Cat# A-21045 RRID:AB_2535714, 1:250) were applied to visualize MyHC expression. Specimens were analyzed using an OLYMPUS confocal microscope (FV1000). CSA was quantified using ImageJ software by an observer blinded to treatment.

2.4.13. Ch25h Promoter Construct

The PGL4.17 plasmid (provided by Dr. Quansheng Zhou, Soochow University) carrying the Ch25h promoter (−300 bp from the start codon), along with a *Renilla* luciferase control reporter (RL-TK) plasmid was transfected into C2C12 cells by lipofectamine 2000 (Invitrogen, Cat# 11668-019). TNF-α (10 ng/ml) was added to the cells 24 h after transfection, and luciferase activity was detected 8 h after the addition of TNF-α by a luminometer (Luminoskan® Ascent, Thermo Scientific).

2.4.14. TUNEL Staining

Frozen sections were fixed by 4% Paraformaldehyde for 20 min at room temperature. After washing between each step, the sections were blocked in 3% H_2O_2 methanol, permeabilized in 0.1% Triton X-100 and then incubated with TUNEL reaction mixture provided by In Situ Cell Death Detection Kit, POD (Roche, Cat# 11684817910). The sections were incubated with DAPI to stain nuclei.

2.4.15. Statistical Analysis

Data were presented as means ± SD. The *t*-test was used to determine the significance of the differences between two groups. Multiple comparisons were analyzed by ANOVA with a post-hoc analysis by the Student-Newman-Keuls test. $P < 0.05$ was considered statistically significant.

3. Results

3.1. Angiotensin II-induced Muscle Wasting is Mediated by TNF-α Signaling Pathway

To address whether TNF-α is a mediator of ang II induced muscle wasting, we infused wild type C57BL/6 or TNFR1KO mice with 500 ng/kg/min ang II or vehicle for 7 days as described previously (Song et al., 2005). In C57BL/6 mice, ang II infusion led to reduced body weight (Fig. 1A), grip strength (Fig. 2A), muscle weight (Fig. 2B–D) and cross sectional area (CSA) of myofibers (Fig. 3A,B), accompanied by elevated serum levels of TNF-α (Fig. 3C). However, ang II induced body weight reduction,

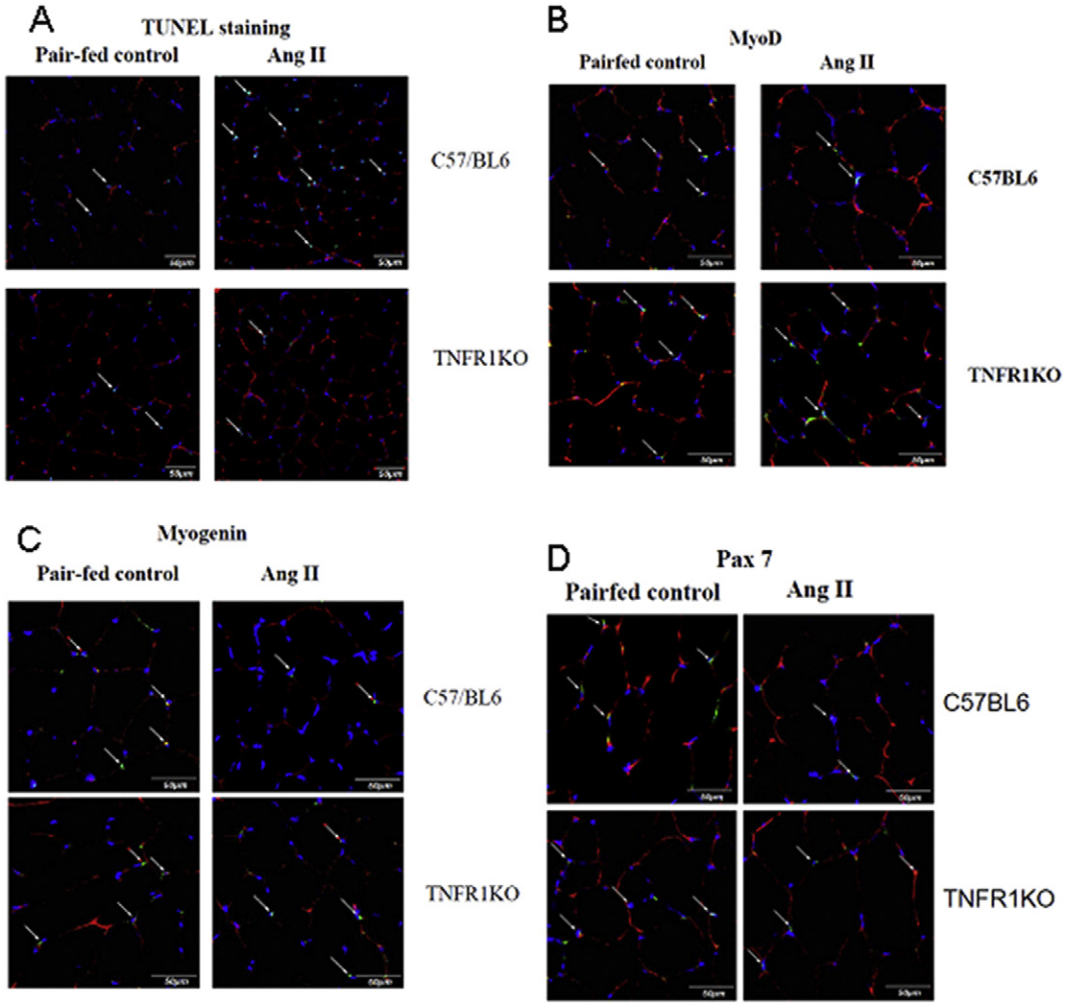

Fig. 5. Ang II infusion leads to increased apoptosis and inhibition of myogenic differentiation in C57BL/6 but not in TNFR1KO mice. (A) TUNEL staining in cryosections of gastrocnemius muscles from ang II infused or pair-fed sham infused C57BL/6 or TNFR1KO mice. (B–D) MyoD, myogenin and Pax 7 staining in cryosections of gastrocnemius muscles from ang II infused or pair-fed sham infused C57BL/6 or TNFR1KO mice. The sections were immunostained with laminin and MyoD, myogenin or Pax7 antibodies, and nuclei were stained with DAPI. The pictures show MyoD, myogenin and Pax7 positive cells (green, indicated by white arrows) and basement membrane outlined by laminin staining (red).

decreased grip strength and muscle loss were prevented in TNFR1KO mice (Figs. 1B, 2–3) despite the increase of TNF-α in the sera of the TNFR1KO mice (Fig. 3C). We performed additional experiments to compare ang II infused mice with ad libitum untreated animals. The results showed decreased body weight, grip strength and muscle weight in ang II infused C57BL/6 mice but not in TNFR1KO mice (Supplementary Figs. 1–2). In contrast to skeletal muscles, the heart weight was increased in ang II infused mice (Supplementary Fig. 3). Our observation is consistent with previous study that heart weights of ang II infused rats were higher than those in controls (Brink et al., 2001).

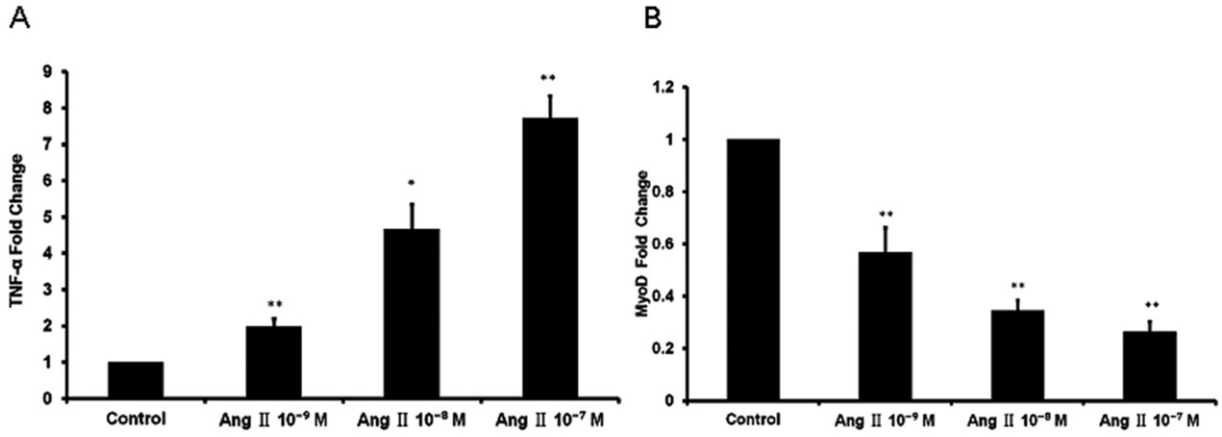

Fig. 6. (A–B) Real-time PCR analysis of TNF-α and MyoD mRNA expression in C2C12 cells treated with ang II. C2C12 cells were cultured in medium containing 2% horse serum in the presence of ang II for 6 days. $^{*}P < 0.05$, $^{**}P < 0.01$, n = 4.

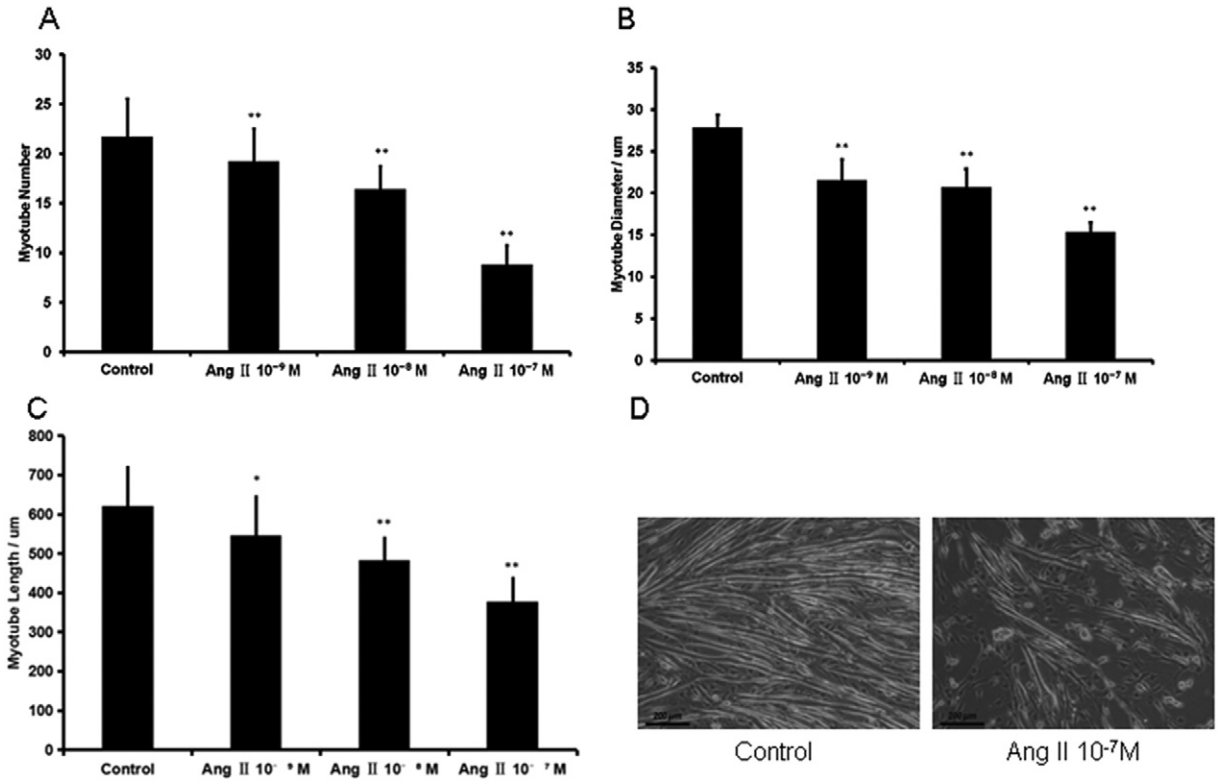

Fig. 7. Ang II inhibits myogenic differentiation in C2C12 cells. (A–C) Myotube number, diameter and length were analyzed in C2C12 cells cultured in medium containing 2% horse serum in the presence of ang II for 6 days. $^{*}P < 0.05$, $^{**}P < 0.01$, n = 3. (D) Representative image of ang II's effect on C2C12 myotube formation.

These findings suggest that TNF-α signaling plays a critical role in ang II induced muscle atrophy. Impaired IGF-1 signaling is a common feature in several wasting conditions. To understand why loss of muscle mass was blunted in TNFR1KO mice, we examined key proteins involved in IGF-1 signaling pathway. Westernblot analysis shows that levels of p-Akt and p-GSK3β were decreased in gastrocnemius muscles from ang II infused wild type C57BL/6, but not from TNFR1KO mice (Fig. 4A–C), suggesting that ang II induced reduction of p-Akt and p-GSK3β is mediated by TNF-α. Reduced phosphorylation of GSK3β leads to its activation, which promotes protein degradation via ubiquitin proteasome pathway (Verhees et al., 2011). We next analyzed expression of atrogin-1 and MuRF1, which are ubiquitin ligases implicated in muscle wasting. Westernblot results showed increased atrogin-1 and MuRF1 expression in the gastrocnemius muscle of C57BL6, but not in TNFR1KO mice (Fig. 4A, D–E), suggesting that ang II induced activation of ubiquitin proteasome pathway is mediated by TNF-α signaling via TNFR1. We have shown previously that caspase-3 mediated apoptosis played a role in ang II induced muscle wasting (Song et al., 2005). We now provide evidence that the expression of cleaved caspase-3 as well as TUNEL positive cells are increased in muscles from ang II infused C57BL/6 mice, but not from TNFR1KO mice (Figs. 4F, 5A). These results suggest that TNF-α is the mediator of ang II induced apoptosis in skeletal muscle. Ang II infusion also caused reduction of MyoD, myogenin and Pax7 expression in wild-type C57BL/6 but not in TNFR1KO mice (Fig. 5B–D), suggesting that myogenic differentiation is impaired by ang II.

3.2. Ch25h is the Downstream Target of TNF-α that Mediate Ang II's Wasting Effect

To explore the mechanisms underlying ang II's wasting effect, we studied the impact of ang II treatment on TNF-α expression using a myoblast line C2C12. Consistent with our in vivo data, ang II treatment resulted in increased expression of TNF-α (Fig. 6A), reduced expression of MyoD (Fig. 6B) and inhibition of myogenic differentiation of both C2C12 cells (Fig. 7) and primary satellite cells (Supplementary Fig. 4). We also isolated satellite cells from ang II treated mice and then cultured the cells in the absence of ang II in order to determine whether inhibitory effect of ang II on satellite cell differentiation can be reversed. Our data showed that the differentiation of satellite cells from ang II treated mice was normal, suggesting that the impairment of myogenic differentiation is 'environment-dependent' (Supplementary Fig. 5). We performed microarray analysis in order to identify genes under TNF-α regulation in C2C12 cells. In response to TNF-α treatment, cholesterol 25-hydroxylase (Ch25h) was upregulated 35.6- and 22.2-fold, in C2C12 cells cultured in 10% FBS and 2% horse serum, respectively (Supplementary Tables 1–2). Real time PCR analysis confirmed microarray findings and showed higher Ch25h mRNA expression compared to microarray results (Fig. 8A). Ch25h is of particular interest because it has been shown previously that 25-hydroxycholeterol (25-OHC), the product of Ch25h, inhibits myoblast fusion (Cornell et al., 1980; Lowrey and Horwitz, 1982), and induces mitochondria-dependent apoptosis via activation of GSK3β (Choi et al., 2008). To define the relationship between TNF-α and Ch25h, we transfected C2C12 cells with a lentivirus over-expressing TNF-α. Overexpression of TNF-α led to inhibition of myogenic differentiation (Fig. 8B), associated with a significant increase of Ch25h mRNA expression (Fig. 9A).

Ch25h catalyzes the formation of 25-OHC from cholesterol. We analyzed the levels of 25-OHC in the serum samples from ang II infused mice by ELISA. The result showed that ang II infusion induced a significant increase of 25-OHC in C57BL/6 but not in TNFR1KO mice (Fig. 9B). Consistent with these findings, ang II treatment increased Ch25h mRNA expression level in C2C12 cells (Fig. 9C).

To assess whether TNF-α affects Ch25h transcription, we transfected C2C12 cells with a plasmid expressing Ch25h-driving luciferase (PGL4.17-Ch25h), along with a control plasmid expressing *Renilla* luciferase (RL-TK). Luciferase assay revealed that Ch25h transcriptional activity increased significantly upon TNF-α stimulation (Fig. 9D). We then constructed a plasmid over-expressing Ch25h in order to

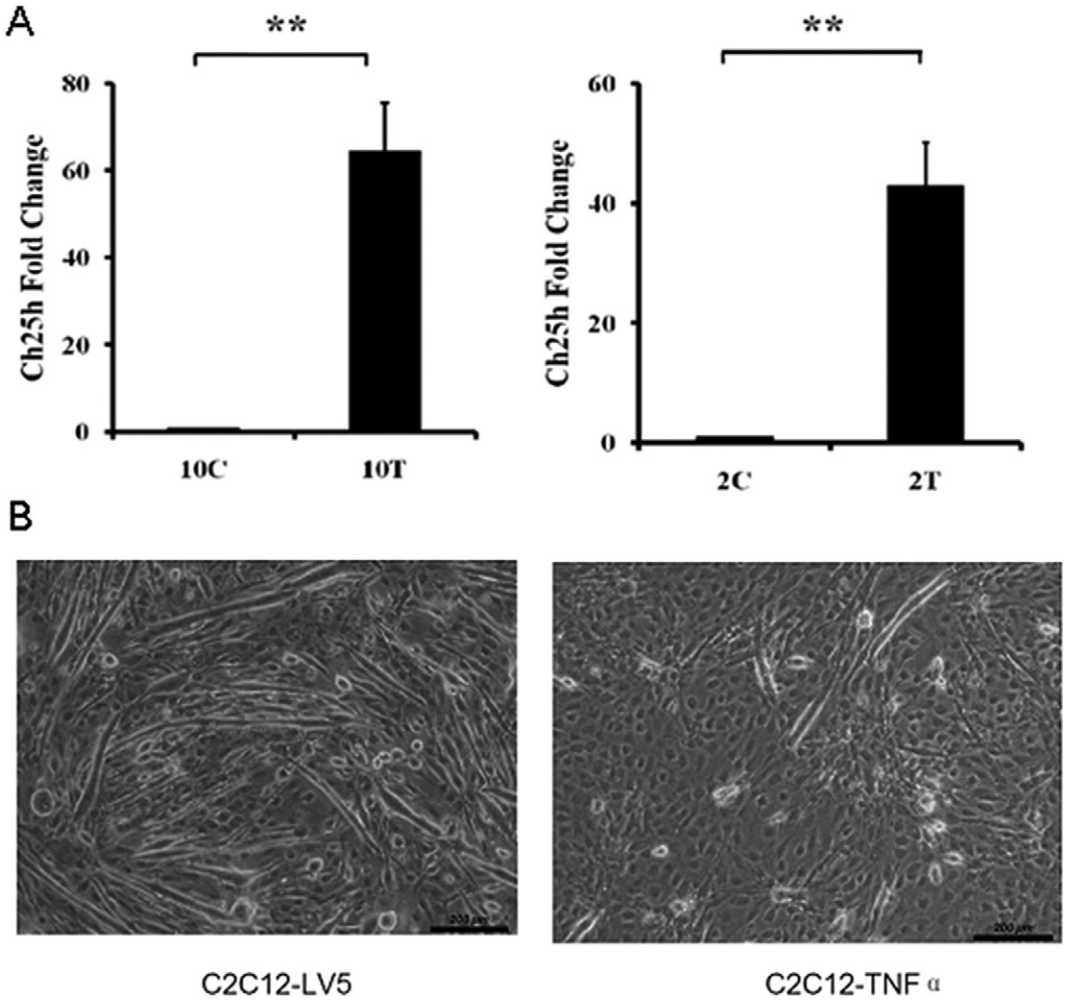

Fig. 8. Ch25h is the down stream target of TNF-α. (A) Real time PCR analysis of Ch25h mRNA levels in C2C12 cells in response to TNF-α treatment. 10C and 2C: C2C12 cells cultured in medium containing 10% FBS (10C) or 2% horse serum (2C), 10T and 2T: C2C12 cells cultured in 10% FBS (10T) or 2% horse serum (2T) treated with TNF-α (50 ng/ml) for 24 h. $^{**}P < 0.01$. n = 3. (B) Representative image of myotube formation in C2C12 cells transfected with lentivirus overexpressing TNF-α or empty vector LV5 (C2C12 cell were cultured in 2% horse serum for 6 days).

investigate the effect of Ch25h expression on muscle wasting. The increased mRNA level of Ch25h in C2C12 cells transfected with Ch25h plasmid was confirmed by real-time PCR (Fig. 10A). Over-expression of Ch25h in C2C12 cells resulted in inhibition of myogenic differentiation (Fig. 10B) and decreased expression of MyoD (Fig. 10C). Furthermore, the mRNA expression levels of atrogin-1 and MuRF1 are increased in C2C12 cells over-expressing Ch25h (Fig. 10D, E). These results show that Ch25h induced muscle wasting is caused by inhibition of myogenic differentiation and activation of the ubiquitin/proteasome pathway.

3.3. 25-OHC Induces Muscle Atrophy via Activation of GSK3β in C57BL/6 Mice

Next, we asked whether 25-OHC could induce muscle wasting in animals. We injected 25-OHC to C57BL/6 mice and found that body and muscle weights were deceased in these mice (Fig. 11). To examine the specificity of the response, 22-OHC and 20-OHC, which are sterols structurally similar to 25-OHC, were also injected to C57BL/6 mice separately. These two sterols did not induce muscle wasting in mice (Fig. 11). It has been shown previously that 25-OHC induces mitochondria-dependent apoptosis via activation of GSK3β and subsequent activation of caspase-3 in PC12 cells (Choi et al., 2008). These previous studies prompted us to determine whether apoptosis plays a role in 25-OHC induced muscle wasting. Westernblot analysis revealed the levels of pAkt, pGSK3β, p-BAD were decreased, whereas levels of cleaved caspase-3 were increased in gastrocnemius muscles from mice received 25-OHC, but not from mice that received 20-OHC, 22-OHC or control treatment (Fig. 12A), suggesting that inactivation of Akt and subsequent activation of GSK3β led to Bad/caspase-3 mediated apoptosis. 25-OHC treatment also resulted in increased expression of atrogin-1 and MuRF1 (Fig. 12A). These results indicate that both ubiquitin-proteosome pathway and apoptosis are involved in 25-OHC induced muscle atrophy. 25-OHC treatment reduced MyoD and Pax7 expression compared to control, 20-OHC and 22R-OHC (Fig. 12B–C), suggesting that myogenic differentiation was impaired by 25-OHC. To further confirm the role of Ch25h in ang II induced muscle loss, we injected lentivirus that overexpress 25-hydroxylase gene into TA muscle of C57BL/6 mice, the contralaterol TA muscles were injected with lenti virus carrying empty vector. The results showed that 25-hydroxylase overexpression in vivo induces muscle atrophy (Fig. 12D). Compared to the control, TA muscles injected with 25-hydroxylase showed reduced expression of MyoD, myogenin, Pax7, but increased TUNEL positive cells (Fig. 13).

3.4. Inhibition of GSK3β Prevents Ang II Induced Muscle Wasting

To determine if a therapeutic strategy might be developed to interfere with muscle wasting when GSK3β is activated, we evaluated TDZD-8, a highly selective small molecule inhibitor of GSK3β that binds to the kinase site of GSK3β. Mice were injected with either

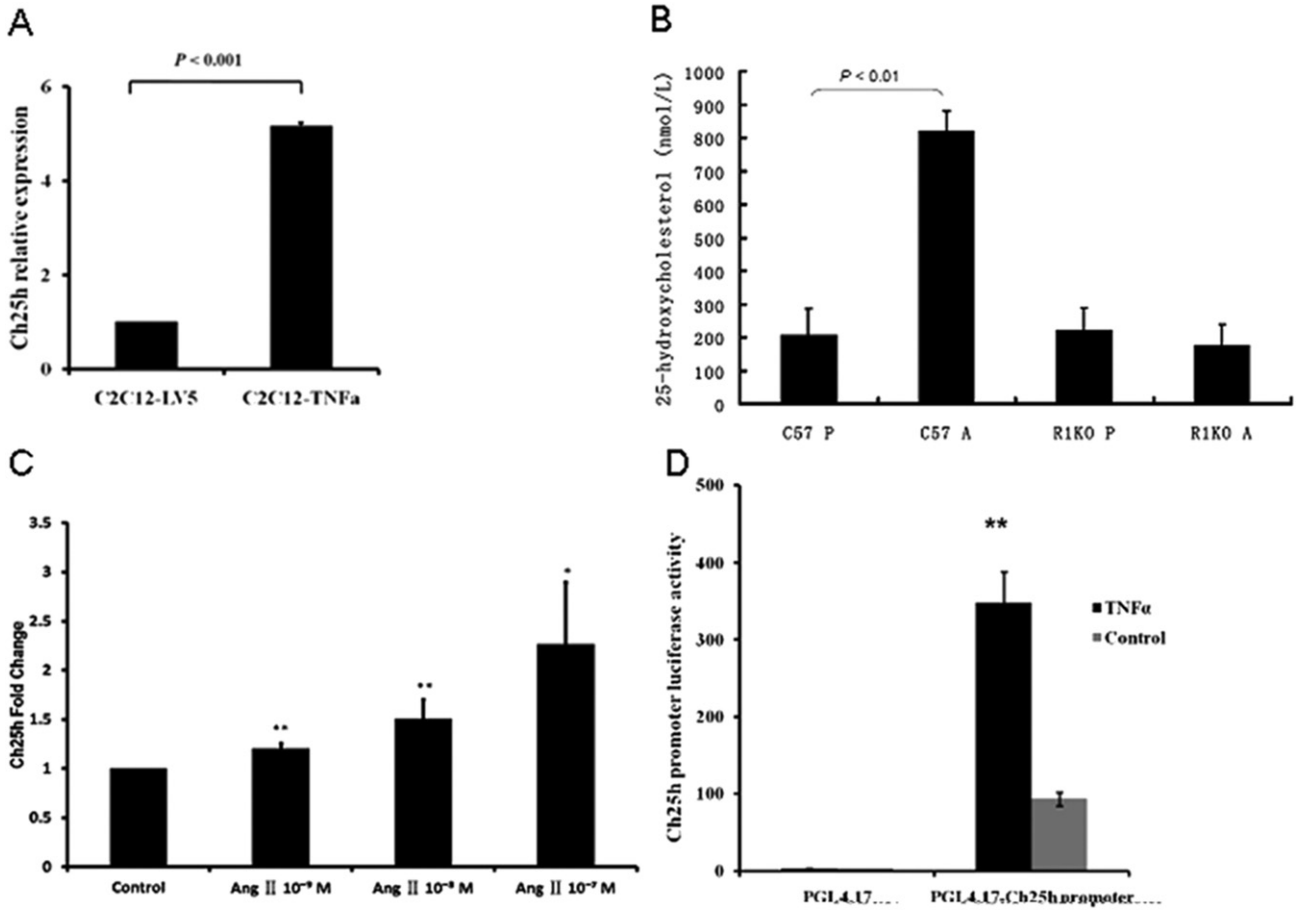

Fig. 9. Ch25h is regulated by ang II induced TNF-α release. (A) Real-time PCR analysis of Ch25h mRNA expression in C2C12 cells cultured in 10% FBS, transfected with either lentivirus over-expressing TNF-α or the empty vector (LV5) were. n = 5. (B) Serum levels of 25-OHC from either ang II (A) or pair-fed sham infused (P) C57BL/6 or TNFR1 knockout mice were measured by ELISA. n = 7 mice/group. (C) Ang II induces expression of Ch25h in C2C12 cells. Real-time PCR analysis of Ch25h mRNA expression in C2C12 cells cultured in 2% horse serum for 6 days in the presence of ang II. n = 3. (D) TNF-α stimulates Ch25h transcriptional activity. C2C12 cells were co-transfected with PGL4.17 plasmid carrying the Ch25h promoter, along with RL-TK plasmid. Twenty-four hours after transfection, the cells were treated with or without TNF-α (10 ng/ml). Dual luciferase activity was measured 8 h after the treatment; n = 3, $^{**}P < 0.01$, TNF-α vs. control.

TDZD-8 or DMSO, and randomly divided into ang II infusion or pair-fed control groups. After 7 days, both body weights and muscle weight were reduced in ang II infused and DMSO treated mice compared to pair-fed control groups (Fig. 14A–D). By contrast, both body weights and muscle weight were preserved in TDZD-8 treated group (Fig. 14A–D). Westernblot analysis showed that ang II induced upregulation of atrogin-1, MuRF1 and caspase-3 cleavage was prevented by TDZD-8 (Fig. 14E).

4. Discussion

Patients with chronic illness such as end stage heart failure, sarcopenia and cancer often develop cachexia, which limit their daily activity and reduces their tolerance to therapy. Cachetic conditions are associated with increased serum angiotensin II (Du Bois et al., 2015; Penafuerte et al., 2016) and TNF-α levels (Martins et al., 2014; Talar-Wojnarowska et al., 2009). Injection of TNF-α reduces the force development in the diaphragm of mice (Mangner et al., 2013). However, the relationship between ang II and TNF-α and their signaling pathways leading to cachexia remain unknown, which hampers the development of effective therapeutic strategies. In the present study, we discovered that TNF-α is the mediator of ang II induced muscle loss and we further identified Ch25h as the down stream molecule that mediates TNF-α's wasting effect. Administration of 25-OHC, the product of Ch25h, induces muscle atrophy in mice through activation of GSK3β signaling pathway. These findings identify 25-OHC as an inducer of muscle atrophy.

Ch25h catalyze the formation of 25-OHC from dietary cholesterol, leading to decreased activity of enzymes involved in cholesterol synthesis. 25-OHC was initially discovered as a regulator of lipid metabolism, and has been implicated in the development of atherosclerosis (Brown and Jessup, 1999). Recent studies indicate that 25-OHC promotes foam cell formation and inflammation (Gold et al., 2014), but the role of 25-OHC in muscle wasting has never been reported before. Evidence for the 25-OHC dependent pathway that initiate loss of muscle mass was obtained from three experimental models: microarray, real-time PCR analysis and luciferase assay confirmed that Ch25h is the down stream target of TNF-α in C2C12 cells; ang II infusion led to the release of 25-OHC in wild type C57BL/6 but not in TNFR1KO mice; 25-OHC injection cause muscle wasting in C57BL/6 mice.

How does 25-OHC influence muscle wasting? Our results show that both ang II infusion and 25-OHC activate GSK3β, which induces muscle loss by three possible mechanisms: (1) activation of ubiquitin/proteasome pathway through inhibition of IGF-1/Akt signaling; (2) activation of mitochondria dependent apoptosis; (3) inhibition of myogenic differentiation.

It has been shown that 25-OHC can block IGF-1 stimulated phosphorylation of Akt and cell survival because 25-OHC inhibits the biosynthesis of cholesterol which is required for activation of IGF-1/Akt pathway (Romanelli et al., 2009). Low p-Akt level causes reduced phosphorylation of GSK3β, which leads to GSK3β activation and subsequent

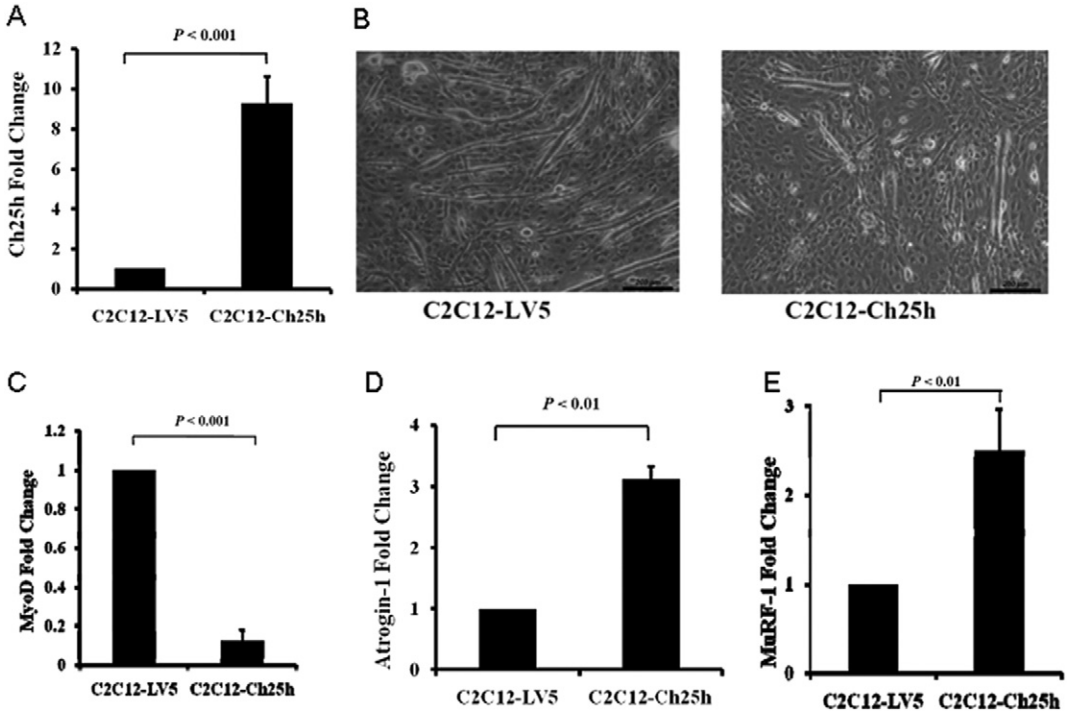

Fig. 10. Ch25h overexpression inhibits myogenic expression and up regulates the expression of atrogin-1 and MuRF-1. (A) Real-time PCR analysis of Ch25h mRNA levels in C2C12 cells transfected with lentivirus over-expressing Ch25h or empty vector LV5. n = 3. (B) Overexpression of Ch25h in C2C12 cells inhibits myogenic differentiation. C2C12 cells transfected with lentivirus over-expressing Ch25h or empty vector LV5 were cultured in medium containing 2% horse serum for 6 days. (C) Real-time PCR analysis of MyoD mRNA levels in C2C12 cells transfected with lentivirus over-expressing Ch25h or empty vector LV5. n = 3. (D–E) Real-time PCR analysis of atrogin-1 and MuRF1 mRNA expression in C2C12 cells transfected with lentivirus over-expressing Ch25h or empty vector LV5.

upregulation of atrogin-1 and MuRF1. Indeed, we found that 25-OHC induced muscle wasting is characterized by reduced levels of p-Akt and p-GSK3β and increased levels of atrogin-1, MuRF-1 and caspase-3, which are in line with our findings from ang II induced muscle wasting. Under physiological conditions, GSK3β is phosphorylated at Ser9 and inactivated by Akt. However, in pathological conditions where IGF-1/Akt signaling is impaired, GSK3β is dephosphorylated at Ser9 and induces muscle loss via up-regulation of atrogin-1, MuRF1 and activation of the ubiquitin-proteasome pathway (Pansters et al., 2015). Activation of GSK-3β is implicated in various forms of muscle wasting including disuse (Pansters et al., 2015) and burn induced muscle loss (Fang et al., 2007). Muscle-specific GSK-3β deletion promotes the recovery of disuse-induced atrophy (Pansters et al., 2015). Pharmacological inhibition of GSK-3β prevents TNF-α induced muscle loss in a guinea pig model of pulmonary inflammation associated muscle atrophy (Verhees et al., 2013). Knockdown of GSK-3β using small interfering RNA suppressed both basal and dexamethasone-induced atrogin-1 and MuRF1 expression in C2C12 myotubes (Verhees et al., 2011). By contrast, activation of GSK-3β leads to up-regulation of atrogin-1/MuRF1 and muscle atrophy (Verhees et al., 2011). Atrogin-1 and

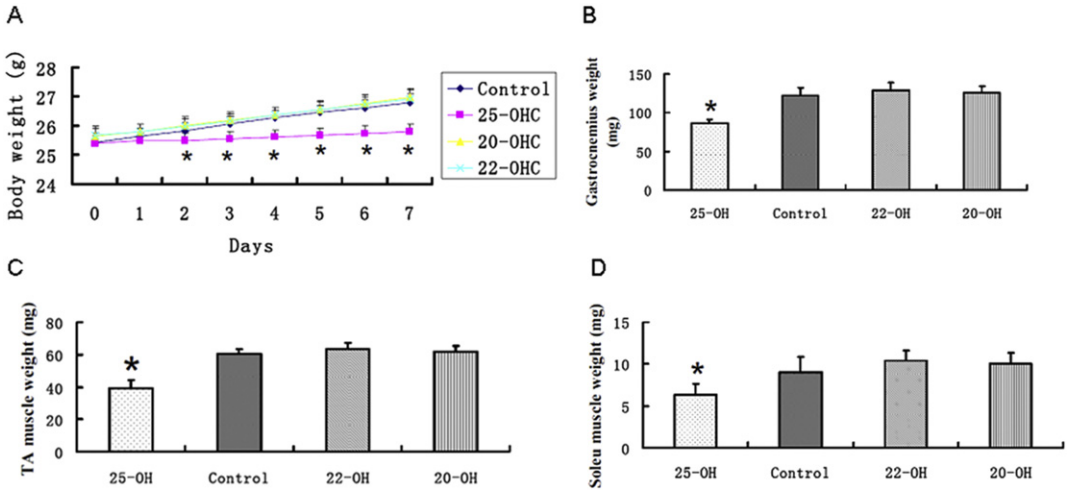

Fig. 11. 25-OHC injection induces muscle wasting in mice. (A) Intraperitoneal injection of 25-OHC, but not 20-OHC, 22-OHC or control solution, resulted in reduction of body weight in C57BL/6 mice. C57BL/6 mice were injected with 25-OHC (25H), control solution containing 0.3% ethanol (Con), 22-OHC (22H), or 20-OHC (20H) daily for 7 days. n = 8 mice/group. *$P < 0.05$. (B–D) Muscle weights from mice described in (A). n = 8 mice/group. *$P < 0.05$.

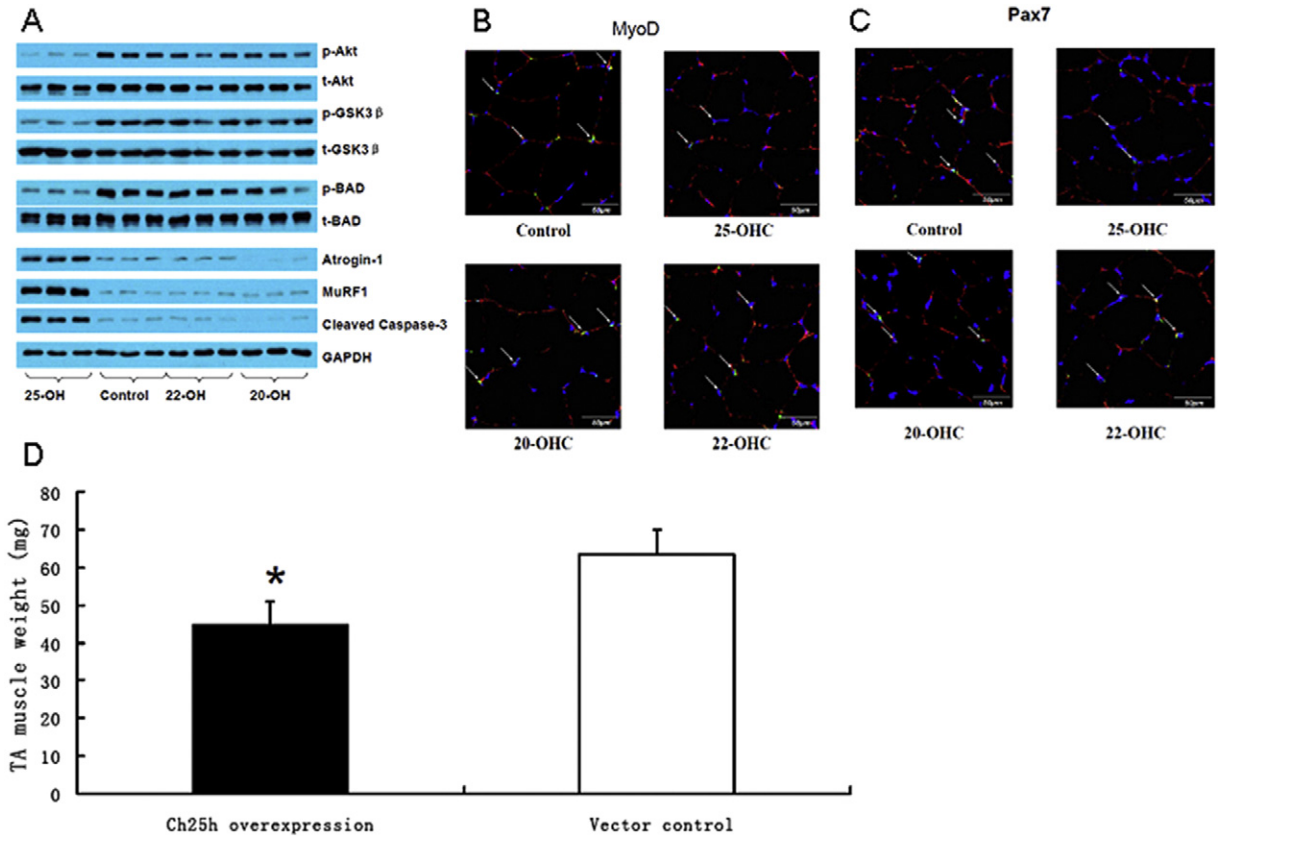

Fig. 12. 25-OHC injection in mice inhibits Akt signaling pathway and the expression of myogenic markers. (A) Representative Westernblots of p-Akt, t-Akt, p-GSK3β, t-GSK3β, p-Bad, t-Bad, atrogin-1, MuRF1, cleaved caspase-3, and GAPDH expression in lysates of gastrocnemius muscles from 25-OHC, control (0.3% ethanol), 22(R)-OHC and 20-OHC treated C57BL/6 mice. n = 3 mice/group. (B–C) Cryosections of gastrocnemius muscles from mice treated with 25-OHC, 20-OHC, 22(R)-OHC or control were immunostained with MyoD or Pax7, and laminin antibodies, and nuclei were stained with DAPI. The pictures show MyoD and Pax7 positive cells (green, indicated by white arrows) and basement membrane outlined by laminin staining (red). (D) Ch25 overexpression induces muscle atrophy in TA muscle. Lentivirus that overexpress 25-hydroxylase gene was injected into TA muscle of C57BL/6 mice, the contralaterol TA muscles were injected with lenti virus carrying empty vector. N = 10 mice/group.

MuRF-1 are E3 ubiquitin ligases which are expressed only in skeletal and smooth muscle cells. These two ubiquitin ligases have been implicated in various types of muscle wasting models and deletion of these genes can prevent muscle atrophy. Our findings that GSK3β inhibitor TDZD-8 pretreatment prevented ang II induced up-regulation of atrogin-1, MuRF-1 and muscle wasting further confirmed the role of GSK3β in mediating ang II's wasting effect. TDZD-8 is a highly specific and potent inhibitor of GSK3β. Previous studies showed that TDZD-8 prevented the increase in atrogin-1 and MuRF1 mRNA levels in dexamethasone-treated myotubes (Evenson et al., 2005), and inhibited protein breakdown in muscles from burned rats (Fang et al., 2005).

Recent studies suggest that activation of GSK3β could also induce apoptosis. In a liver ischemia reperfusion (IR) model, TDZD-8 treatment prevented IR induced caspase-3 activation and apoptosis (Rocha et al., 2015), suggesting a role of GSK3β in mediating the activation of caspase-3 dependent apoptotic pathway. Suppression of GSK-3β activation by M-cadherin protects myoblasts against mitochondria-associated apoptosis during myogenic differentiation (Wang et al., 2011). Inactivation of GSK-3β facilitates recovery of mitochondria potential by suppressing ROS production, leading to cytoprotection from oxidant stress-induced cell death (Sunaga et al., 2014). Along this line, ang II infusion was shown to induce ROS production and mitochondria dependent apoptosis in mouse skeletal muscle (Kadoguchi et al., 2015). Bad is an important protein involved in mitochondrial dependent apoptosis. Bad induces apoptosis by displacing Bax from binding to Bcl-2. Once dissociated from Bcl-2, Bax will translocate into mitochondria and triggers the release of cytochrome *c*. Anti-apoptotic factors such as IGF-1 inhibits the apoptotic activity of Bad by activating Akt, which phosphorylates Bad at Ser136. Our data suggest that 25-OHC induced muscle atrophy may be partially mediated by mitochondria dependent apoptosis through de-phosphorylation and activation of Bad. 25-OHC was shown to induce apoptosis in macrophages through activation of Bad by degrading Akt (Rusinol et al., 2004). We now provided evidence that 25-OHC injection resulted in reduced levels of p-Bad and increased levels of cleaved caspase-3 in mouse gastrocnemius muscles. In addition to activation of Bad, 25-OHC has also been shown to induce apoptosis in cardiomyocytes, smooth muscle cells, and PC-12 cells via the production of reactive oxygen species and activation of GSK3β (Appukuttan et al., 2013; Choi et al., 2008; Lee da et al., 2015; Rosca et al., 2012; Sekiya et al., 2014).

GSK3β is a negative regulator of muscle differentiation and growth, and its knockdown stimulates myogenic differentiation of skeletal muscle cells (van der Velden et al., 2008). Pharmacological inhibition of GSK3β attenuates TNF-α and glucocorticoid induced suppression of MyoD expression and myotube formation in C2C12 and primary satellite cells (Ma et al., 2014; Verhees et al., 2013). TDZD-8 also improved muscle strength and Pax7 expression (a marker for satellite cells) in HSA^{LR} mice, a mouse model of myotonic dystrophy (Jones et al., 2012). These studies suggest that GSK3β inhibits muscle regeneration by inhibiting activation of satellite cells. Indeed, our in vivo data showed reduced MyoD expression in muscles from mice received either ang II

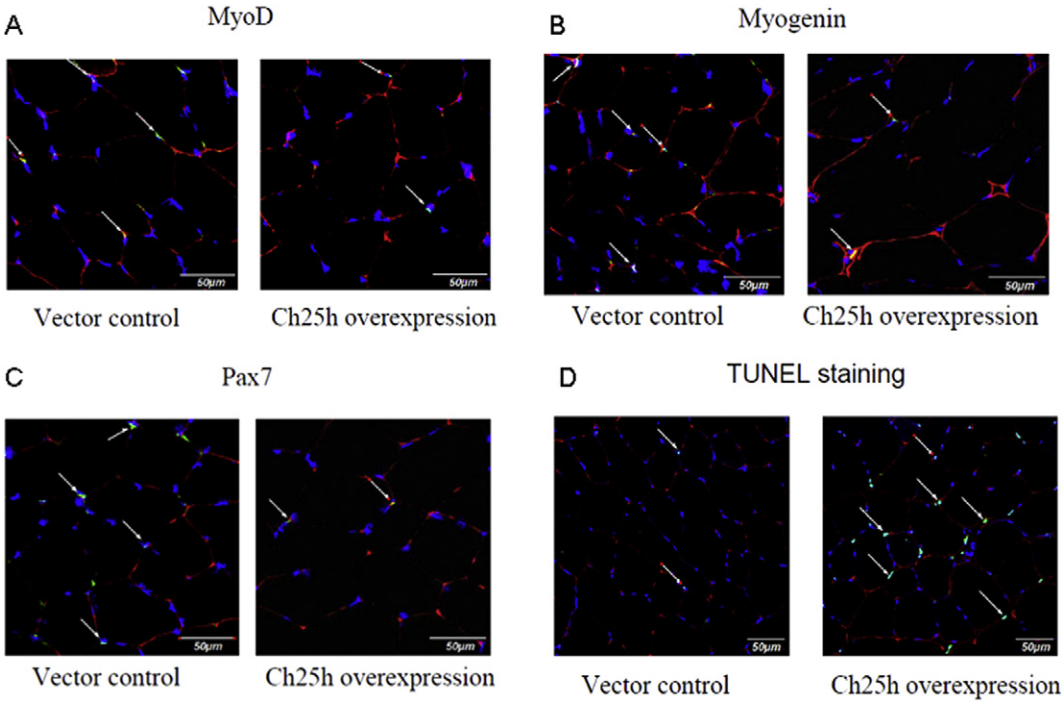

Fig. 13. Ch25 overexpression in TA muscle inhibits the expression of myogenic markers and induces apoptosis. (A–C) Cryosections of TA muscles injected with lentivirus overexpressing 25-hydroxylase gene or lenti virus carrying empty vector were immunostained with MyoD, myogenin or Pax7, and laminin antibodies, and nuclei were stained with DAPI. (D) TUNEL staining in cryosections of TA muscles injected with lentivirus that overexpress 25-hydroxylase gene or lenti virus carrying empty vector.

infusion or 25-OHC, accompanied by reduced expression levels of p-GSK3β. These results demonstrate that 25-OHC induced muscle wasting is mediated in part by inhibition of myogenic differentiation via activation of GSK3β.

How could ang II stimulate the production of 25-OHC? A previous study demonstrated that transcription and translation of Ch25h are increased in response to TNF-α in glioblastoma cell lines (Eibinger et al., 2013). Indeed, our results showed that serum levels of 25-OHC were

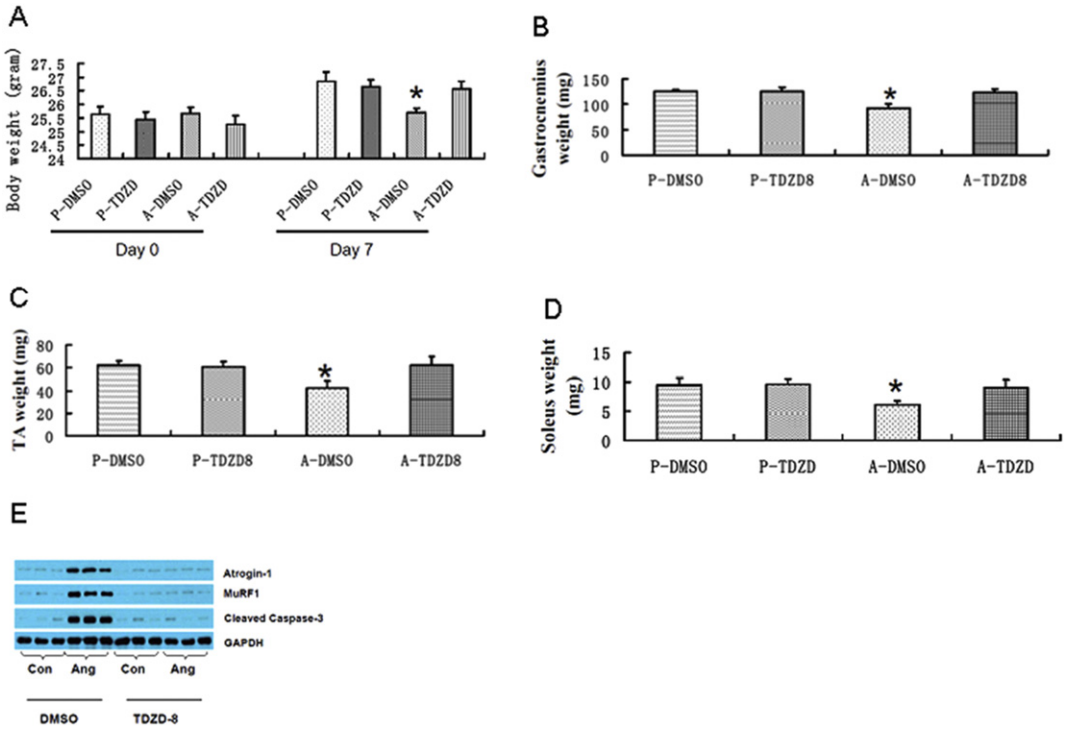

Fig. 14. GSK3β inhibitor TDZD-8 prevents ang II induced muscle wasting. (A) Body weight at day 0 and day 7. Mice were either ang II infused or pair-fed sham infused following TDZD or DMSO treatment. n = 7 mice/group. *$P < 0.05$. (B–D) Muscle weight from C57BL/6 mice treated with either TDZD-8 or DMSO. Mice were either ang II infused or pair-fed sham infused following TDZD or DMSO treatment. n = 7 mice/group. *$P < 0.05$. (E) Representative Westernblots of atrogin-1, MuRF1, cleaved caspase-3 and GAPDH expression in lysates of gastrocnemius muscles of C57BL/6 mice treated with TDZD-8. Mice were either ang II infused (ang) or pair-fed sham infused (con) following TDZD-8 or DMSO injections. n = 3 mice/group.

increased in ang II infused wild type C57BL/6 mice, but not in ang II infused TNFR1KO mice, suggesting that ang II induced secretion of 25-OHC is mediated by TNF-α signaling through TNFR1. Luciferase assay confirmed that Ch25h transcriptional activity increased significantly upon TNF-α stimulation in C2C12 cells.

Our results have identified a pathway that stimulates muscle wasting in response to ang II. The pathway is mediated by TNF-α through its type 1 receptor and subsequent activation of Ch25h and release of 25-OHC, which in turn impairs Akt signaling, leading to activation of GSK3β. Previous studies have shown that ang II not only contribute to cardiac cachexia, but also play an important role in muscle wasting associated with sarcopenia and cancer. Age-related increase in ang II level contributes to the development of sarcopenia. Losartan, an ang II type I receptor blocker significantly improved exercise capacity in aged mice (Lin et al., 2014) and prevented disuse atrophy in aged mice that were subjected to hindlimb immobilization (Burks et al., 2011). Animal studies showed that ACE inhibitor could attenuate weight loss in mice bearing MAC16 tumor (Sanders et al., 2005). Clinical studies showed that cancer cachexia is associated with elevated plasma levels of ang II (Penafuerte et al., 2016). Therefore, our work laid the foundation for exploiting Ch25h as a target for the development of specific therapies for treating cachexia associated with heart failure, sarcopenia and cancer.

Funding Sources

This work was supported by the National Natural Science Foundation of China (81670358 to YHS. Nos. 81120108003, 81330007), Jiangsu Province Key Scientific and Technological Project (BE2016669), the project for the Priority Academic Program Development of Jiangsu Higher Education Institutions (PAPD), Suzhou Science and Technology Project (SS201665).

Conflicts of Interest

The authors declare no conflicts of interest.

Author Contributions

Conception and design of the study: C.C.S., J.Z., C.L., B.L., X.Y.Y., X.P., Y.L., Y.H.S.

Acquisition of data, or analysis and interpretation of data: C.C.S., J.Z., X.X.W., C.L., B.L., X.Y.Y., X.P., Q.Z., J.S., J.J.W., M.Y.B., C.F.W., Y.L., Y.H.S.

Drafting the article or revising it critically for important intellectual content: C.C.S., J.Z., Y.L., Y.H.S.

Final approval of the version to be submitted: all authors.

Acknowledgement

We thank Dr. Min-Sheng Zhu from Nanjing University for providing technical support in isolating satellite cells.

Appendix A. Supplementary data

Supplementary data to this article can be found online at http://dx.doi.org/10.1016/j.ebiom.2017.01.040.

References

Appukuttan, A., Kasseckert, S.A., Kumar, S., Reusch, H.P., Ladilov, Y., 2013. Oxysterol-induced apoptosis of smooth muscle cells is under the control of a soluble adenylyl cyclase. Cardiovasc. Res. 99, 734–742.

Brink, M., Price, S.R., Chrast, J., Bailey, J.L., Anwar, A., Mitch, W.E., Delafontaine, P., 2001. Angiotensin II induces skeletal muscle wasting through enhanced protein degradation and down-regulates autocrine insulin-like growth factor I. Endocrinology 142, 1489–1496.

Brown, A.J., Jessup, W., 1999. Oxysterols and atherosclerosis. Atherosclerosis 142, 1–28.

Burks, T.N., Andres-Mateos, E., Marx, R., Mejias, R., Van Erp, C., Simmers, J.L., Walston, J.D., Ward, C.W., Cohn, R.D., 2011. Losartan restores skeletal muscle remodeling and protects against disuse atrophy in sarcopenia. Sci. Transl. Med. 3, 82ra37.

Choi, Y.K., Kim, Y.S., Choi, I.Y., Kim, S.W., Kim, W.K., 2008. 25-hydroxycholesterol induces mitochondria-dependent apoptosis via activation of glycogen synthase kinase-3beta in PC12 cells. Free Radic. Res. 42, 544–553.

Cicoira, M., Bolger, A.P., Doehner, W., Rauchhaus, M., Davos, C., Sharma, R., Al-Nasser, F.O., Coats, A.J., Anker, S.D., 2001. High tumour necrosis factor-alpha levels are associated with exercise intolerance and neurohormonal activation in chronic heart failure patients. Cytokine 15, 80–86.

Cornell, R.B., Nissley, S.M., Horwitz, A.F., 1980. Cholesterol availability modulates myoblast fusion. J. Cell Biol. 86, 820–824.

Dalla Libera, L., Ravara, B., Angelini, A., Rossini, K., Sandri, M., Thiene, G., Battista Ambrosio, G., Vescovo, G., 2001. Beneficial effects on skeletal muscle of the angiotensin II type 1 receptor blocker irbesartan in experimental heart failure. Circulation 103, 2195–2200.

Doehner, W., Bunck, A.C., Rauchhaus, M., von Haehling, S., Brunkhorst, F.M., Cicoira, M., Tschope, C., Ponikowski, P., Claus, R.A., Anker, S.D., 2007. Secretory sphingomyelinase is upregulated in chronic heart failure: a second messenger system of immune activation relates to body composition, muscular functional capacity, and peripheral blood flow. Eur. Heart J. 28, 821–828.

Du Bois, P., Pablo Tortola, C., Lodka, D., Kny, M., Schmidt, F., Song, K., Schmidt, S., Bassel-Duby, R., Olson, E.N., Fielitz, J., 2015. Angiotensin II induces skeletal muscle atrophy by activating TFEB-mediated MuRF1 expression. Circ. Res. 117, 424–436.

Eibinger, G., Fauler, G., Bernhart, E., Frank, S., Hammer, A., Wintersperger, A., Eder, H., Heinemann, A., Mischel, P.S., Malle, E., Sattler, W., 2013. On the role of 25-hydroxycholesterol synthesis by glioblastoma cell lines. Implications for chemotactic monocyte recruitment. Exp. Cell Res. 319, 1828–1838.

Evenson, A.R., Fareed, M.U., Menconi, M.J., Mitchell, J.C., Hasselgren, P.O., 2005. GSK-3beta inhibitors reduce protein degradation in muscles from septic rats and in dexamethasone-treated myotubes. Int. J. Biochem. Cell Biol. 37, 2226–2238.

Fang, C.H., Li, B.G., James, J.H., King, J.K., Evenson, A.R., Warden, G.D., Hasselgren, P.O., 2005. Protein breakdown in muscle from burned rats is blocked by insulin-like growth factor i and glycogen synthase kinase-3beta inhibitors. Endocrinology 146, 3141–3149.

Fang, C.H., Li, B., James, J.H., Yahya, A., Kadeer, N., Guo, X., Xiao, C., Supp, D.M., Kagan, R.J., Hasselgren, P.O., Sheriff, S., 2007. GSK-3beta activity is increased in skeletal muscle after burn injury in rats. Am. J. Physiol. Regul. Integr. Comp. Physiol. 293, R1545–R1551.

Gold, E.S., Diercks, A.H., Podolsky, I., Podyminogin, R.L., Askovich, P.S., Treuting, P.M., Aderem, A., 2014. 25-Hydroxycholesterol acts as an amplifier of inflammatory signaling. Proc. Natl. Acad. Sci. U. S. A. 111, 10666–10671.

Hardin, B.J., Campbell, K.S., Smith, J.D., Arbogast, S., Smith, J., Moylan, J.S., Reid, M.B., 2008. TNF-alpha acts via TNFR1 and muscle-derived oxidants to depress myofibrillar force in murine skeletal muscle. J. Appl. Physiol. 104, 694–699.

Jones, K., Wei, C., Iakova, P., Bugiardini, E., Schneider-Gold, C., Meola, G., Woodgett, J., Killian, J., Timchenko, N.A., Timchenko, L.T., 2012. GSK3beta mediates muscle pathology in myotonic dystrophy. J. Clin. Invest. 122, 4461–4472.

Kadoguchi, T., Kinugawa, S., Takada, S., Fukushima, A., Furihata, T., Homma, T., Masaki, Y., Mizushima, W., Nishikawa, M., Takahashi, M., Yokota, T., Matsushima, S., Okita, K., Tsutsui, H., 2015. Angiotensin II can directly induce mitochondrial dysfunction, decrease oxidative fibre number and induce atrophy in mouse hindlimb skeletal muscle. Exp. Physiol. 100, 312–322.

Khawaja, T., Chokshi, A., Ji, R., Kato, T.S., Xu, K., Zizola, C., Wu, C., Forman, D.E., Ota, T., Kennel, P., Takayama, H., Naka, Y., George, I., Mancini, D., Schulze, C.P., 2014. Ventricular assist device implantation improves skeletal muscle function, oxidative capacity, and growth hormone/insulin-like growth factor-1 axis signaling in patients with advanced heart failure. J. Cachexia Sarcopenia Muscle 5, 297–305.

Lee da, H., Nam, Y.J., Lee, M.S., Sohn, D.S., Lee, C.S., 2015. Rotundarpene attenuates cholesterol oxidation product-induced apoptosis by suppressing the mitochondrial pathway and the caspase-8- and bid-dependent pathways. Eur. J. Pharmacol. 749, 39–48.

Lin, C.H., Yang, H., Xue, Q.L., Chuang, Y.F., Roy, C.N., Abadir, P., Walston, J.D., 2014. Losartan improves measures of activity, inflammation, and oxidative stress in older mice. Exp. Gerontol. 58, 174–178.

Liu, J., Liang, X., Zhou, D., Lai, L., Xiao, L., Liu, L., Fu, T., Kong, Y., Zhou, Q., Vega, R.B., Zhu, M.S., Kelly, D.P., Gao, X., Gan, Z., 2016. Coupling of mitochondrial function and skeletal muscle fiber type by a miR-499/Fnip1/AMPK circuit. EMBO Mol. Med. 8, 1212–1228.

Llovera, M., Garcia-Martinez, C., Lopez-Soriano, J., Carbo, N., Agell, N., Lopez-Soriano, F.J., Argiles, J.M., 1998. Role of TNF receptor 1 in protein turnover during cancer cachexia using gene knockout mice. Mol. Cell. Endocrinol. 142, 183–189.

Lowrey, C.H., Horwitz, A.F., 1982. Effect of inhibitors of cholesterol synthesis on muscle differentiation. Biochim. Biophys. Acta 712, 430–432.

Ma, Z., Zhong, Z., Zheng, Z., Shi, X.M., Zhang, W., 2014. Inhibition of glycogen synthase kinase-3beta attenuates glucocorticoid-induced suppression of myogenic differentiation in vitro. PLoS One 9, e105528.

Mancini, D.M., Walter, G., Reichek, N., Lenkinski, R., McCully, K.K., Mullen, J.L., Wilson, J.R., 1992. Contribution of skeletal muscle atrophy to exercise intolerance and altered muscle metabolism in heart failure. Circulation 85, 1364–1373.

Mangner, N., Linke, A., Oberbach, A., Kullnick, Y., Gielen, S., Sandri, M., Hoellriegel, R., Matsumoto, Y., Schuler, G., Adams, V., 2013. Exercise training prevents TNF-alpha induced loss of force in the diaphragm of mice. PLoS One 8, e52274.

Martins, T., Vitorino, R., Moreira-Goncalves, D., Amado, F., Duarte, J.A., Ferreira, R., 2014. Recent insights on the molecular mechanisms and therapeutic approaches for cardiac cachexia. Clin. Biochem. 47, 8–15.

Pansters, N.A., Schols, A.M., Verhees, K.J., de Theije, C.C., Snepvangers, F.J., Kelders, M.C., Ubags, N.D., Haegens, A., Langen, R.C., 2015. Muscle-specific GSK-3beta ablation

accelerates regeneration of disuse-atrophied skeletal muscle. Biochim. Biophys. Acta 1852, 490–506.
Penafuerte, C.A., Gagnon, B., Sirois, J., Murphy, J., MacDonald, N., Tremblay, M.L., 2016. Identification of neutrophil-derived proteases and angiotensin II as biomarkers of cancer cachexia. Br. J. Cancer 114, 680–687.
Rocha, J., Figueira, M.E., Barateiro, A., Fernandes, A., Brites, D., Pinto, R., Freitas, M., Fernandes, E., Mota-Filipe, H., Sepodes, B., 2015. Inhibition of glycogen synthase kinase-3beta attenuates organ injury and dysfunction associated with liver ischemia-reperfusion and thermal injury in the rat. Shock 43, 369–378.
Romanelli, R.J., Mahajan, K.R., Fulmer, C.G., Wood, T.L., 2009. Insulin-like growth factor-I-stimulated Akt phosphorylation and oligodendrocyte progenitor cell survival require cholesterol-enriched membranes. J. Neurosci. Res. 87, 3369–3377.
Rosca, A.M., Matei, C., Dragan, E., Burlacu, A., 2012. Cardiomyocyte apoptosis in ischaemia-reperfusion due to the exogenous oxidants at the time of reperfusion. Cell Biol. Int. 36, 1207–1215.
Rusinol, A.E., Thewke, D., Liu, J., Freeman, N., Panini, S.R., Sinensky, M.S., 2004. AKT/protein kinase B regulation of BCL family members during oxysterol-induced apoptosis. J. Biol. Chem. 279, 1392–1399.
Sanders, P.M., Russell, S.T., Tisdale, M.J., 2005. Angiotensin II directly induces muscle protein catabolism through the ubiquitin-proteasome proteolytic pathway and may play a role in cancer cachexia. Br. J. Cancer 93, 425–434.
Sekiya, M., Yamamuro, D., Ohshiro, T., Honda, A., Takahashi, M., Kumagai, M., Sakai, K., Nagashima, S., Tomoda, H., Igarashi, M., Okazaki, H., Yagyu, H., Osuga, J., Ishibashi, S., 2014. Absence of Nceh1 augments 25-hydroxycholesterol-induced ER stress and apoptosis in macrophages. J. Lipid Res. 55, 2082–2092.
Song, Y.H., Li, Y., Du, J., Mitch, W.E., Rosenthal, N., Delafontaine, P., 2005. Muscle-specific expression of IGF-1 blocks angiotensin II-induced skeletal muscle wasting. J. Clin. Invest. 115, 451–458.
Sunaga, D., Tanno, M., Kuno, A., Ishikawa, S., Ogasawara, M., Yano, T., Miki, T., Miura, T., 2014. Accelerated recovery of mitochondrial membrane potential by GSK-3beta inactivation affords cardiomyocytes protection from oxidant-induced necrosis. PLoS One 9, e112529.
Talar-Wojnarowska, R., Gasiorowska, A., Smolarz, B., Romanowicz-Makowska, H., Kulig, A., Malecka-Panas, E., 2009. Tumor necrosis factor alpha and interferon gamma genes polymorphisms and serum levels in pancreatic adenocarcinoma. Neoplasma 56, 56–62.
Toth, M.J., Ades, P.A., Tischler, M.D., Tracy, R.P., LeWinter, M.M., 2006. Immune activation is associated with reduced skeletal muscle mass and physical function in chronic heart failure. Int. J. Cardiol. 109, 179–187.
van der Velden, J.L., Schols, A.M., Willems, J., Kelders, M.C., Langen, R.C., 2008. Glycogen synthase kinase 3 suppresses myogenic differentiation through negative regulation of NFATc3. J. Biol. Chem. 283, 358–366.
Verhees, K.J., Schols, A.M., Kelders, M.C., Op den Kamp, C.M., van der Velden, J.L., Langen, R.C., 2011. Glycogen synthase kinase-3beta is required for the induction of skeletal muscle atrophy. Am. J. Physiol. Cell Physiol. 301, C995–C1007.
Verhees, K.J., Pansters, N.A., Baarsma, H.A., Remels, A.H., Haegens, A., de Theije, C.C., Schols, A.M., Gosens, R., Langen, R.C., 2013. Pharmacological inhibition of GSK-3 in a guinea pig model of LPS-induced pulmonary inflammation: II. Effects on skeletal muscle atrophy. Respir. Res. 14, 117.
von Haehling, S., Doehner, W., Anker, S.D., 2007. Nutrition, metabolism, and the complex pathophysiology of cachexia in chronic heart failure. Cardiovasc. Res. 73, 298–309.
Wang, Y., Hao, Y., Alway, S.E., 2011. Suppression of GSK-3beta activation by M-cadherin protects myoblasts against mitochondria-associated apoptosis during myogenic differentiation. J. Cell Sci. 124, 3835–3847.
Yende, S., Waterer, G.W., Tolley, E.A., Newman, A.B., Bauer, D.C., Taaffe, D.R., Jensen, R., Crapo, R., Rubin, S., Nevitt, M., Simonsick, E.M., Satterfield, S., Harris, T., Kritchevsky, S.B., 2006. Inflammatory markers are associated with ventilatory limitation and muscle dysfunction in obstructive lung disease in well functioning elderly subjects. Thorax 61, 10–16.
Zhou, H., Ge, Y., Sun, L., Ma, W., Wu, J., Zhang, X., Hu, X., Eaves, C.J., Wu, D., Zhao, Y., 2014. Growth arrest specific 2 is up-regulated in chronic myeloid leukemia cells and required for their growth. PLoS One 9, e86195.